Interaction of the C2 Domain from Protein Kinase Cϵ with Model Membranes†

Sonia Sánchez-Bautista, Ana de Godos, José A. Rodríguez-Alfaro, Alejandro Torrecillas, Senena Corbalán-García, and Juan C. Gómez-Fernández*

Departamento de Bioquímica y Biología Molecular (A), Facultad de Veterinaria, Universidad de Murcia, Apartado de Correos 4021, E-30080 Murcia, Spain

Received October 18, 2006; Revised Manuscript Received December 22, 2006

ABSTRACT: The C2 domain from protein kinase Cϵ (PKCϵ) binds to membranes but does not require Ca^{2+} to do so. This work examines the mode in which the conformation and organization of the phospholipids present in model membranes are altered by the presence of the C2 domain from PKCϵ (C2-PKCϵ). It is concluded from the results of differential scanning calorimetry that the protein shifted the temperature of the gel to the fluid phase transition of pure 1-palmitoyl-2-oleoyl-*sn*-glycero-3-phosphate (POPA), widening the transition and increasing it to a higher temperature. When POPA was mixed with 1-palmitoyl-2-oleoyl-*sn*-glycero-3-phosphocholine (POPC), the changes in the transition were smaller and no phase separation was observed. Experiments performed using magic angle spinning NMR showed that this C2 domain specifically affected POPA when the phospholipid was mixed with POPC, as indicated by the downfield shift in the isotropic resonance of POPA, the widening of the resonance peak, the decrease in T_2, and the decrease in T_1 observed at all temperatures. All these effects were quite marked compared with the very small effect observed with POPC, indicating the specificity of the effect. The presence of the C2-PKCϵ protein changed the conformation of the polar head group of POPA, as shown by infrared spectroscopy. All these results clearly illustrate the electrostatic interaction that takes place between this C2 domain and membranes which contain POPA in the absence of Ca^{2+}.

The protein kinase Cϵ (PKCϵ)[1] isoenzyme, which belongs to the group of novel PKCs, has been linked with the regulation of several biological processes, including neuron differentiation (*1*, *2*), antiviral resistance (*3*), hormone secretion (*4*), transporter regulation (*5*, *6*), and integrin-dependent signaling (*7*, *8*). In addition, PKCϵ has been described as being responsible for the regulation of both cell survival and apoptosis in various cellular systems, whereas it protected MCF-7 cells from tumor necrosis factor α (TNFα)-induced apoptosis (*9*) and promoted the survival of lung cancer cells (*10*). In contrast, PKCϵ has been shown to mediate neuronal death induced by oxidative stress (*11*) and the apoptosis of macrophages in response to lipopolysaccharide via c-*Jun* NH_2-terminal kinase (JNK) activation (*10*). PKCϵ also plays an important role as a mediator of cellular tolerance to ischemeic stress of the heart (*12*, *13*), and the demonstration of a striking PKCϵ cardioprotective phenotype in diabetic psiepsilon-RACK (epsilon-agonist) mice is very interesting in this respect (*14*). It has been shown, in fact, that it is possible to obtain cardioprotection from ischemia by continuous delivery of a protein kinase Cϵ-activating peptide (*15*).

Novel PKCs possess a regulatory part consisting of a C1 domain, which binds diacylglycerol or phorbol esters, and a C2 domain which does not bind Ca^{2+}. PKCs bind to membranes mainly through electrostatic interactions, due to their recognition of negative charge phospholipids, such as phosphatidylserine or phosphatidic acid (*16*−*18*). It is well-known that zwitterionic phospholipids, such as phosphatidylcholine, are not suitable for the electrostatic interaction of peripheral charged proteins with membranes (*19*). Structural studies have shown that the C2 domain of classical PKCs such as PKCα exhibits two areas at the top surface of the molecule which might participate in its binding to anionic membranes (*16*−*18*). In vitro experiments have confirmed the ability of both the C2 domain and full-length PKCϵ to bind to negatively charged phospholipid vesicles in a Ca^{2+}-independent manner, which is similar to what is seen in the case of other novel PKC isoenzymes (*20*−*24*). It has also been shown that this C2 domain has a preference for phosphatidic acid (*22*, *23*) and that phosphatidic acid is an important and essential activator of PKCϵ in vivo through the C2 domain (*25*). Of note is the fact that although phosphatidic acid has a very simple polar group, it is still a very active bioactive lipid and is specifically recognized by many proteins (*26*).

The recent description of the importance of the C2 domain for the translocation of PKCϵ to membranes in vivo and the role played by phosphatidic acid in the translocation (*25*)

† This work was supported by grants from the Dirección General de Investigación (BFU2005-02482) and Fundación Séneca, Región de Murcia (00591/P1/04).

* To whom correspondence should be addressed. Telephone: +34-968-364766. Fax: +34-968-364766. E-mail: jcgomez@um.es.

[1] Abbreviations: C2-PKCϵ, C2 domain from PKCϵ; DSC, differential scanning calorimetry; ΔH_{cal}, calorimetric enthalpy; fwhh, full width at half-height; MAS, magic angle spinning; MLV, multilamellar vesicles; POPA, 1-palmitoyl-2-oleoyl-*sn*-glycero-3-phosphate; PKCϵ, protein kinase Cϵ; POPC, 1-palmitoyl-2-oleoyl-*sn*-glycero-3-phosphocholine; T_c, temperature of the phase transition onset; T_m, temperature of the maximum C_p of the transition; $T_{1/2}$, width of the transition at half-height; T_1, ^{31}P spin−lattice relaxation time; T_2, ^{31}P spin−spin relaxation time.

10.1021/bi0621720 CCC: $37.00
Published on Web 02/15/2007

suggest that the domain binds to lipids as a complement to protein−protein interaction and that PKCϵ may be regulated by the signaling pathway triggered by phospholipase D.

Magic angle spinning (MAS) NMR is a very helpful technique for studying large membrane vesicles since it provides high-resolution spectra (*27*, *28*) without the need to sonicate vesicles, meaning that model membranes, which are more similar to biomembranes, may be used. ^{31}P NMR, in particular, permits the direct observation of the phosphate group of phospholipids in high-resolution spectra so that the different phospholipids present in multilamellar vesicles may be resolved (*29*) and changes in their isotropic chemical shifts and relaxation times following their perturbation by proteins may be determined (*29*−*33*). We also used differential scanning calorimetry (DSC) to show that the protein affects the membrane but does not lead to phase separation. Finally, when infrared spectroscopy was used to study the interaction of the protein with the lipid−water interface, it was demonstrated that the protein modifies the conformation of the head group of the phospholipids.

MATERIALS AND METHODS

Sample Preparation. Lipids were obtained from Avanti Polar Lipids (Alabaster, AL).

The C2 domain from PKCϵ was prepared as previously described (*23*). Briefly, the cDNA fragment corresponding to residues 1−138 of the rat PKCϵ C2 domain, a kind gift from Drs. Nishizuka and Ono (Kobe University, Kobe, Japan), was amplified using PCR. The resulting 414 bp fragment was subcloned into the HindIII and BamHI sites of the pET28a(+) bacterial expression vectors, where the inserts were N-terminally fused to a tag of six histidines (6His). All constructs were confirmed by DNA sequencing. Variants of C2-PKCϵ were generated by PCR site-directed mutagenesis (*34*).

The pET28a(+) plasmid containing C2-PKCϵ was expressed and purified as previously described (*21*, *23*). Basically, the plasmids were transformed into *Escherichia coli* BL21(DE3) cells. The bacterial cultures ($OD_{600} = 0.6$) were induced for 5 h at 30 °C with 0.5 mM isopropyl 1-thio-β-D-galactopyranoside (IPTG) (Roche). The cells were lysed by sonication in lysis buffer [25 mM HEPES (pH 7.4) and 100 mM NaCl] containing protease inhibitors (10 mM benzamidine, 1 mM PMSF, and 10 μg/mL trypsin inhibitor). The soluble fraction of the lysate was incubated with Ni-NTA agarose (QIAGEN, Hilden, Germany) for 2 h at 4 °C. The Ni beads were washed with lysis buffer containing 20 mM imidazole. The bound fractions were eluted with the same buffer containing 250 mM imidazole. The 6His tag was removed after thrombin cleavage, and finally, C2-PKCϵ was desalted and concentrated using an Ultrafree-5 centrifugal filter unit (Millipore Inc., Bedford, MA). The protein concentration was determined using the BCA method (*35*). The M_r of this protein is 15 608.7 Da.

Lipid vesicles (MLV) were generated by mixing chloroform solutions of 1-palmitoyl-2-oleoyl-*sn*-glycero-3-phosphocholine (POPC) and/or 1-palmitoyl-2-oleoyl-*sn*-glycero-3-phosphate (POPA) in the desired proportions and then dried from the organic solvent under a nitrogen stream and further dried under vacuum for 60 min. The dried phospholipids were resuspended in buffer containing 25 mM Hepes (pH 7.4) and 0.5 mM EGTA by vigorous vortexing to produce multilayered vesicles. When protein was also present, it was added in the buffer used to resuspend the lipids so that the final lipid:protein molar ratio was 40:1.

Solid State NMR Measurements. ^{31}P MAS NMR experiments were carried out on a Bruker Avance 600 instrument (Bruker, Etlingen, Germany) operating at proton frequencies of 600.13 and 242.9 MHz for ^{31}P. A double-resonance 4 mm MAS broadband probe from Bruker was used for ^{31}P observation under proton decoupling at high potency. The spectra were acquired at a spinning speed of 4 kHz. Spectra of 1352 data points were obtained with a spectral width of 19 380 Hz, an acquisition time of 0.034 s, and a recycle time of 5 s. Spectra were zero-filled at 16 384 points and 2 Hz line boadening. To obtain the one-dimensional MAS ^{31}P spectra, a 5 μs pulse was used with gated decoupling of ^{1}H. In the T_1 experiments, the inversion−recovery method was used, with ^{1}H decoupling and 10 different delay times. In the T_2 experiment, the cpmg method was used (Carr−Purcell−Meiboom−Gill) with ^{1}H uncoupling, and 10 spectra were acquired with different repetition cycles.

To prepare samples for NMR experiments, MLV liposomes prepared as described in the previous paragraph, with or without protein, were spun down at 14 000 rpm for 30 min, and the resulting pellets were introduced into 4 mm NMR zirconia rotors.

Differential Scanning Calorimetry. A high-sensitivity MicroCal (Northampton, MA) VP scanning calorimeter was used in these experiments. Scan rates were 60°/h, and low-temperature mode was used. Samples (160 μL) contained 1 mg of phospholipids and the protein necessary to give a lipid:protein molar ratio of 40:1. These lipid/protein mixtures were resuspended in 25 mM Hepes (pH 7.4) and 0.5 mM EGTA. Multilayered vesicles were generated by vigorous mixing. A buffer profile was subtracted from the sample scans. Baselines were created by the cubic spline and subtracted. The calorimetric parameters T_c (temperature of the phase transition onset), T_m (temperature of the maximum C_p of the transition), $T_{1/2}$ (width of the transition at half-height), and ΔH_{cal} (calorimetric enthalpy) were extracted from the data and processed with Origin 5.0 (MicroCal).

Infrared Spectroscopy. Multilayered lipid vesicles (MLV) were prepared as described above for NMR, in the presence and absence of the proteins. H_2O buffer was used to obtain samples for the phosphate region and D_2O buffer for samples for the other regions of the spectrum. Centrifugation provided pellets formed of the vesicles in the bottom of the tube when H_2O buffer was used but which floated when D_2O buffer was used. Lipid vesicles were recovered from either the pellets or the floating layers and deposited on the infrared windows.

Infrared spectra were recorded using a Bruker Vector 22 Fourier transform infrared spectrometer equipped with an MCT detector. Samples were examined in a thermostated Specac 20710 cell (Specac, Kent, U.K.) equipped with CaF_2 windows and 6 μm spacers (H_2O buffer) or 25 μm spacers (D_2O buffer). The spectra were recorded after the samples were equilibrated at the desired temperature for 10 min in the infrared cell. A total of 128 scans were carried out for each spectrum with a nominal resolution of 2 cm^{-1} and then Fourier transformed using a triangular apodization function. A sample shuttle accessory was used to obtain the average

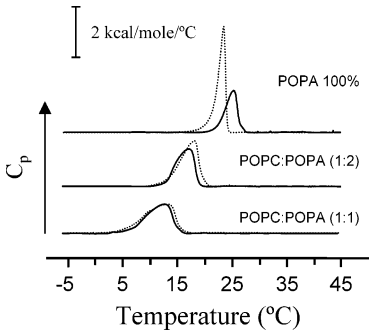

FIGURE 1: DSC thermograms for phospholipid vesicles with different compositions, as indicated: 100% POPA, POPC/POPA (1:2 molar ratio), and POPC/POPA (1:1 molar ratio) in the absence (···) and in the presence of C2-PKCϵ (—).

background and sample spectra. The sample chamber of the spectrometer was continuously purged with dry air to prevent atmospheric water vapor from obscuring the bands of interest. Infrared spectroscopy of aqueous samples can be used to study biological samples by spectral subtraction, which allows the subtraction of the water spectral contribution (*36*). Spectral processing was carried out in general as described previously (*37*). Briefly, spectral subtraction was performed interactively using Grams/32 (Galactic Industries Corp., Salem, NH). Derivation gave the number and position, as well as an estimation of the bandwidth and intensity of the bands making up the phospholipid carbonyl region. Thereafter, curve fitting was performed, and the heights, widths, and positions of each band were optimized successively. The fractional areas of the bands in this region were calculated from the final fitted band areas.

RESULTS

DSC Measurements. When C2-PKCϵ was added to pure POPA, the endothermic peak corresponding to the phase transition shifted to a higher temperature so that, whereas the T_c transition temperature of the pure lipid was 16 °C, the T_c for the lipid−protein complex was 19.6 °C (Figure 1 and Table 1). In addition, ΔH decreased from 7.6 to 4.6 kcal/mol, and the full width at half-height ($T_{1/2}$) of the transition also increased from 1.4 to 2.5 °C in width (Table 1). When mixtures of phospholipids, including POPC and POPA (1:2 molar ratio) or POPC and POPA (2:1 molar ratio), were used, the effect of the protein on all ΔH, T_c, T_m, and $T_{1/2}$ was very small (Figure 1 and Table 1). It should be noticed that the molar ratio was 40:1 (lipid/protein), and it is unlikely that one C2-PKCϵ molecule could interact at the same time with more than a few phospholipid molecules; however, no phase separation between POPA and POPC was produced by the addition of protein to the POPC/POPA mixtures.

^{31}P MAS NMR. High-resolution solid state ^{31}P MAS NMR was used to obtain information about the interaction between C2-PKCϵ and the phospholipids present in the model membranes. First, it was thought that the results may provide general information about the type of interaction and, additionally, since POPC and POPA can be resolved in the spectra, specific information might also be obtained. ^{31}P NMR may provide information about the local electrostatic environment for each lipid species of those present in the membrane.

Figure 2 shows ^{31}P MAS NMR spectra for multilamellar vesicles of POPA and different POPC/POPA mixtures at 30 °C. The spectra of vesicles differing in phospholipid composition were studied in the presence and absence of C2-PKCϵ. Under MAS conditions, high-resolution spectra were obtained and the individual phospholipids could be observed. It was interesting that the spectral lines were narrow, reflecting the fact that membranes were in a fluid state at 30 °C. Table 2 shows the isotropic ^{31}P NMR chemical shift values of the different phospholipid vesicles and the values of fwhh for each resonance peak.

In the case of the pure POPA sample, a single resonance peak was observed with a chemical shift of 1.21 ppm and a fwhh of 0.13 ppm (Figure 2A and Table 2). When C2-PKCϵ was added to the POPA MLV system at a 40:1 phospholipid:protein molar ratio, the peak shifted and the chemical shift was now 1.91 ppm with a fwhh of 0.40 ppm (Figure 2A and Table 2). This downfield shift in the isotropic resonance of POPA is clearly related to the association of the protein with the lipid. Similar changes in ^{31}P NMR chemical shift were observed previously as a consequence of the association of cardiotoxin II with POPG, the shift being attributed to the interaction of the phospholipid headgroups with cationic sites on the protein, deshielding the phosphorus nucleus (*30*). A downfield displacement of chemical shift has been shown to occur as the phosphoryl group of phosphatidic acid loses its proton and takes on a second negative charge (*38*, *39*). In other systems, like that of the Aβ_{1-40} peptide, it was found that the ^{31}P NMR resonance of dimyristylphosphatidylcholine and dimyristylphosphatidylglycerol shifted upfield (*31*, *40*) probably because of the different type of phospholipid involved, in which case the change in the conformation of the polar head group may be different from that occurring in phosphatidic acid.

Another consequence of the binding of C2-PKCϵ to the POPA vesicles is a widening of the resonance peak, the increase in the fwhh clearly reflecting a decrease in phospholipid mobility. A widening of this type has previously been observed for dimyristylphosphatidylglycerol in the presence of the Aβ_{1-40} peptide, when it was also interpreted as a restriction in the mobility of the phospholipid (*31*).

In another experiment, the mutant PKCϵ-C2W23A/R26A/R32A was used, also at a 40:1 phospholipid:protein molar ratio. This mutant was previously shown to possess a reduced capacity to bind to POPA (*23*). Figure 2A demonstrates that the downfield shift of the ^{31}P NMR resonance of POPA was less pronounced than that observed in the presence of the wild-type protein, shifting to only 1.61 ppm, while the fwhh increased to only 0.33 ppm (Table 2).

Additionally, POPC was introduced into the membrane composition, thus reducing the surface charge of the membranes due to POPA. First, a POPC/POPA mixture at a 1:2 molar ratio was used to prepare MLVs. Figure 2B shows that two clearly resolved isotropic resonance peaks were now observed at −0.51 (POPC) and 0.71 ppm (POPA), the relative size of the peaks reflecting the molar ratio. It was interesting that the resonance peak from POPA was shifted upfield, compared with that of pure POPA (1.21 ppm). In the same way, when the POPC:POPA molar ratio was 1:1 (Figure 2 and Table 2), the resonance peak from POPA was further shifted upfield to 0.51 ppm. The same trend was also observed in the POPC/POPA (2:1) sample with a value of

Table 1: Values of Different Thermodynamic Parameters for the Chain Melting Transition of Different Phospholipid Mixtures (molar ratios indicated) in the Absence and Presence of the C2 Domain from PKCϵ[a]

	POPA	C2ϵ with POPA	PC/PA (1:2)	C2ϵ with PC/PA (1:2)	PC/PA (1:1)	C2ϵ with PC/PA (1:1)
ΔH (kcal/mol)	7.6	4.6	7.7	6.0	7.7	6.7
T_c (°C)	16.0	19.6	9.1	10.3	0.8	2.5
T_m (°C)	23.5	25.3	18.1	17.1	13.3	12.7
$T_{1/2}$ (°C)	1.4	2.5	3.8	4.0	6.4	5.5

[a] T_c values correspond to the onset of the transition, T_m values to the temperature of the maximum of the transition endothermic peak, and $T_{1/2}$ values to the width of the transition peak at half-height.

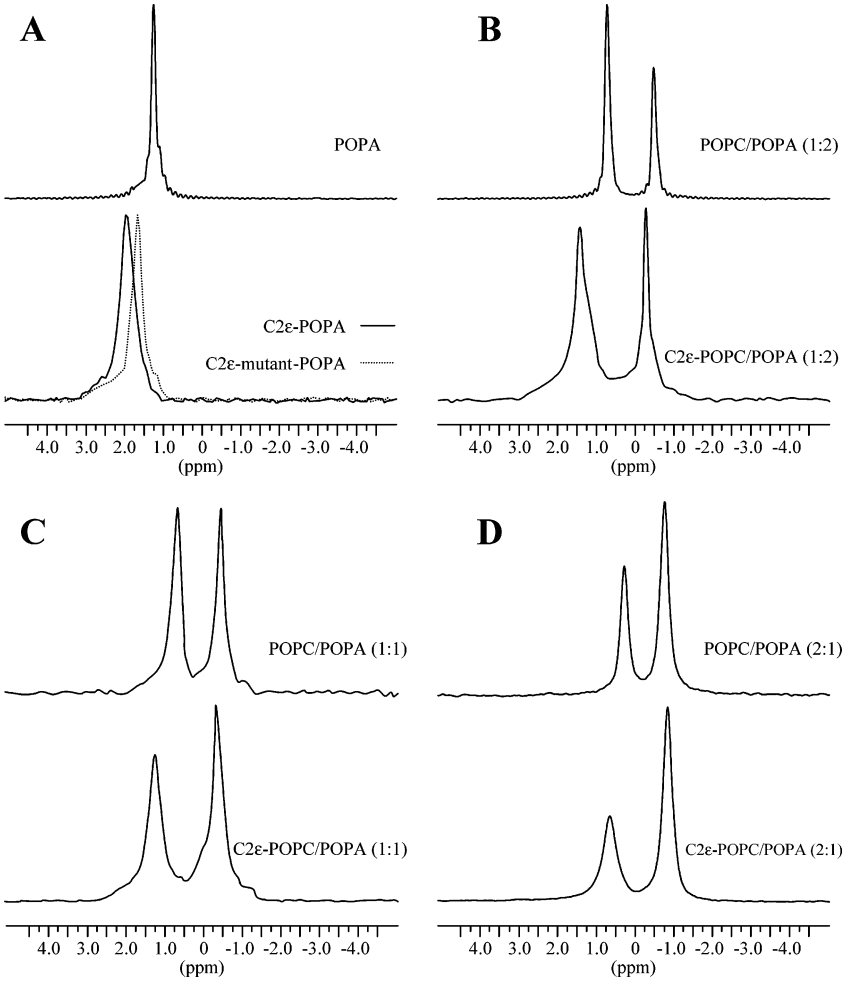

FIGURE 2: ^{31}P MAS NMR spectra from MLV suspensions containing pure POPA and different POPA/POPC compositions, in the absence and presence of C2-PKCϵ: (A) pure POPA (top) and POPA with C2-PKCϵ (bottom). POPA with the mutant PKCϵ-C2W23A/R26A/R32A is shown with a dashed line. (B) POPC/POPA (1:2 molar ratio) in the absence (top) and presence of C2-PKCϵ (bottom). (C) POPC/POPA (1:1 molar ratio) in the absence (top) and presence of C2-PKCϵ (bottom). (D) POPC/POPA (2:1 molar ratio) in the absence (top) and presence of C2-PKCϵ (bottom). The MAS speed was kept at 4 kHz and the temperature at 30 °C.

0.33 ppm for POPA (Figure 2D). This effect, which was modified by a parallel decrease in surface charge, has been observed by other authors using dimyristylphosphatidylcholine/dimyristylphosphatidylglycerol mixtures and attributed to the change in the electrostatic potential present at the membrane surface (*31*, *40*). As previously described, when phosphatidic acid is mixed with phosphatidylcholine, the phosphatidylcholine molecules keep the charged phosphatidic acid headgroups apart, reducing the surface charge density on the membrane and thus yielding a lower apparent pK_a (*38*). Since the chemical shift changed upfield when phosphatidic acid becomes protonated (*38*, *39*), it is clear that the inclusion of POPC molecules increases the degree of protonation of POPA. Note that the isotropic resonance from POPC shifted downfield when POPA was included in the membrane, reaching −0.51 ppm in the POPC/POPA mixture (1:2 molar ratio) (Figure 2B and Table 2) compared with −0.91 ppm in pure POPC, −0.62 ppm in the POPC/POPA sample at a 1:1 molar ratio (Figure 2C), and −0.79 ppm in the POPC/POPA sample (2:1 molar ratio) (Figure 2D).

The incorporation of C2-PKCϵ in POPC/POPA vesicles, at a 40:1 phospholipid:protein molar ratio, resulted in downfield changes in chemical shifts, especially in the case of the POPA resonance. In the POPC/POPA (1:2 molar ratio) sample, the ^{31}P NMR resonance peak corresponding to POPA appeared at 1.32 ppm (0.71 ppm in the absence of protein)

Table 2: ^{31}P MAS NMR Chemical Shifts and Full Widths at Half-Height (fwhh) for Different Phospholipid Mixtures (molar ratios indicated) in the Absence and Presence of the C2 Domain from PKCϵ[a]

	^{31}P from POPC		^{31}P from POPA	
	chemical shift (ppm)	fwhh (ppm)	chemical shift (ppm)	fwhh (ppm)
POPA			1.21	0.13
C2ϵ with POPA			1.91	0.40
C2ϵ mutant with POPA			1.61	0.33
POPC/POPA (1:2)	−0.51	0.13	0.71	0.13
C2ϵ with POPC/POPA (1:2)	−0.40	0.13	1.32	0.40
POPC/POPA (1:1)	−0.62	0.21	0.51	0.13
C2ϵ with POPC/POPA (1:1)	−0.41	0.32	1.21	0.40
POPC/POPA (2:1)	−0.79	0.27	0.33	0.24
C2ϵ with POPC/POPA (2:1)	−0.86	0.27	0.61	0.40
POPC	−0.91	0.15		
C2ϵ with POPC	−0.82	0.17		

[a] The C2ϵ mutant corresponds to PKCϵ-C2W23A/R26A/R32A. The values corresponding to the ^{31}P from POPC and from POPA can be examined separately due to the resolution afforded by the MAS technique.

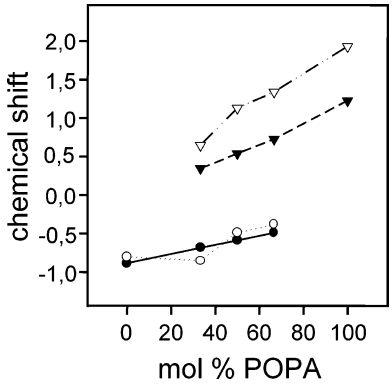

FIGURE 3: Isotropic ^{31}P chemical shift values at 30 °C for POPC/POPA MLV suspensions vs the mole percent of POPA in the absence (▼ and ●) and presence (▽ and ○) of C2-PKCϵ. The circles correspond to the ^{31}P from POPC and the triangles to ^{31}P from POPA.

and the resonance corresponding to POPC appeared at −0.40 ppm (−0.51 ppm in the absence of protein) (see Figures 2A and 3). In the POPC/POPA (1:1 molar ratio) sample, the POPA resonance was found at 1.21 ppm (0.51 ppm in the absence of protein) and that corresponding to POPC at −0.41 ppm (−0.62 ppm in the absence of protein) (see Figure 2C and Table 2). A considerable widening of the resonances was observed as a consequence of the addition of the protein in the POPC/POPA (1:2 molar ratio) sample (Figure 2B and Table 2), which especially affected the POPA resonance. This underlined the stronger interaction of the protein with POPA; the fwhh for the POPA peak increased to 0.40 ppm, whereas that from the POPC peak remained at 0.13 ppm. In the POPC/POPA (1:1 molar ratio) sample, however, the resonances from both phospholipids were widened, with a fwhh of 0.40 ppm being recorded for POPA and a fwhh of 0.32 for POPC (Figure 2C and Table 2). In the POPC/POPA (2:1 molar ratio) sample, the resonance from POPA exhibited a chemical shift of 0.61 ppm (0.33 ppm, in the absence of protein) and that from POPC a shift to −0.86 ppm (−0.79 ppm in the absence of protein) (Figure 2D and Table 2).

In an additional control experiment in which protein was added to pure POPC (Table 2 and Figure 3), very little

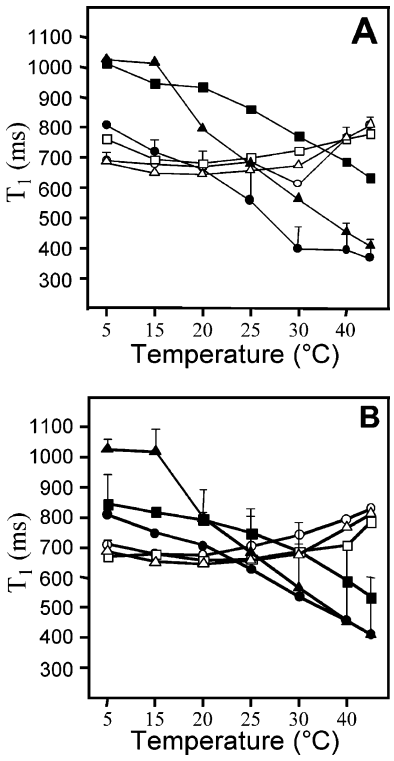

FIGURE 4: ^{31}P MAS NMR longitudinal relaxation times, T_1, from MLVs. Pure POPC (△) and pure POPA (▲) are shown in both parts. (A) POPC/POPA at a 1:2 molar ratio. ^{31}P from POPC in the absence (□) and presence (○) of C2-PKCϵ and ^{31}P from POPA in the absence (■) and in the presence (●) of C2-PKCϵ. POPC/POPA at 2:1 molar ratio. ^{31}P from POPC in the absence (□) and in the presence (○) of C2-PKCϵ and ^{31}P from POPA in the absence (■) and in the presence (●) of C2-PKCϵ. T_1 values are shown as a function of temperature.

change was observed, the POPC resonance shifting from −0.91 ppm in the absence of protein to −0.82 ppm in its presence. This confirms that the membrane−protein interaction involves electrostatic interaction and that POPC cannot facilitate this type of interaction because of its zwitterionic nature. Figure 3 clearly shows a much steeper slope for the curve of POPA than for that of the POPC samples, again indicating the specific interaction of C2-PKCϵ with negatively charged membranes.

^{31}P Relaxation. The ^{31}P spin−lattice relaxation times, T_1, of each phospholipid in the membrane were simultaneously determined from the high-resolution MAS NMR spectra, which were obtained at different temperatures (Figure 4).

When pure POPA was studied (Figure 4A), the first two temperatures (5 and 15 °C) produced very similar T_1 values of 1026 and 1016 ms, respectively. However, when the temperature was increased to 25 °C, the T_1 fell abruptly to 796 ms. As the temperature rose further, T_1 values decreased, gradually reaching 409 ms at 60 °C. The abrupt change occurring after the first two temperatures were very probably related to the gel to fluid phase transition temperature which occurs with a T_c of 16 °C in POPA (Figure 1).

In the case of pure POPC (Figure 4A), all the measurements were taken above its gel to fluid phase transition (−4 °C), and any changes with increasing temperatures were not as pronounced as with POPA. It can be seen (Figure 4A) that the minimum (645 ms) occurred at ∼25 °C. The minimum values observed by other authors in the ^{31}P T_1

versus temperature plot for phospholipids such as POPC were ~15 °C for dioleoylphosphatidylcholine bilayers (*41*), 0 °C for cardiolipin bilayers (*42*), 25 °C for bilayers of dioleoylphosphatidylserine (*43*), 15 °C for dioleoylphosphadylserine (*29*), 18 °C for dioleoylphosphatidylglycerol (*29*), and 37 °C for diacylphosphatidylinositol (*29*). All these phospholipids have T_1 minima around 800−1000 ms. This T_1 relaxation time minimum is a value which provides an unambiguous view of the nuclei since it is not necessary to know the exact relaxation mechanism to evaluate the correlation time for the molecular motion at the temperature of the minimum T_1 (*42*). This T_1 minimum was not however observed for POPA, at least in the range of temperatures that was studied, although the presence of a gel phase at low temperatures may have impeded this observation.

It was thought that it might be interesting to observe the effect of mixing POPC and POPA in the bilayer. As can be seen, in a POPC/POPA (1:2 molar ratio) sample (Figure 4A), the data corresponding to the ^{31}P from POPA contained only one point (5 °C), which is below the gel to fluid phase transition (17 °C), while from 15 to 60 °C, there was a progressive and linear decline from 1016 to 419 ms. Figure 4A clearly shows that in the fluid phase the T_1 relaxation times of POPA (for example, 560 ms at 55 °C) were clearly longer than those recorded for pure POPA (470 ms at 55 °C) (Figure 4A), perhaps because POPC molecules are arranged among the POPA molecules. Waltham et al. (*44*) reported that phosphatidic acid molecules establish hydrogen bonding between their phosphate groups. This bonding network will be disrupted by the presence of POPC molecules, reducing the surface charge density on the membrane and leading to a change in the phosphate group conformation of the POPA molecules, which will be reflected in higher T_1 values (Figure 4A). Indeed, this effect can be observed in both POPC/POPA (1:2) (Figure 4A) and POPC/POPA (2:1, molar ratio) (Figure 4B) mixtures. In the presence of C2-PKCϵ, however, the T_1 values of POPA were shifted at all temperatures toward lower values, in both samples (see panels A and B of Figure 4). This reduction in T_1 would be the result of the presence of the protein electrostatically interacting with the negatively charged surface of the membrane.

Similar results have already been seen for the binding of other basic proteins to membranes containing phosphatidic acid and other negatively charged phospholipids. For example, this type of effect was observed for cytochrome *c*, when it was interpreted as being caused by restrictions of the headgroup motion that lower the spectral density of fast motions (on the 10^{-9} s time scale) of the phosphorus atom, as a consequence of binding to the protein (*45*). Other basic proteins which have been shown to reduce the T_1 values of ^{31}P of negatively charged phosholipids are poly(L-lysine), myelin basic protein, lysozyme, and ribonuclease (*46*).

Finally, it should be noted that only very small effects were observed for the T_1 values of POPC as a result of the presence of either POPA or POPA with protein (Figure 4A,B), underlining their very low susceptibility to electrostatic interactions.

Spin−spin relaxation times (T_2) were measured for the POPC/POPA (1:1 molar ratio) sample, in the absence and presence of C2-PKCϵ, and a 40:1 lipid:protein molar ratio, and the results showed a decrease in T_2 values. T_2 values were 22.3 and 22.6 ms for POPA and POPC, respectively, in the absence of protein and 11.35 and 16.4 ms, respectively, in its presence. These increases agreed fairly well with the observed widening of the isotropic resonances (see Table 2).

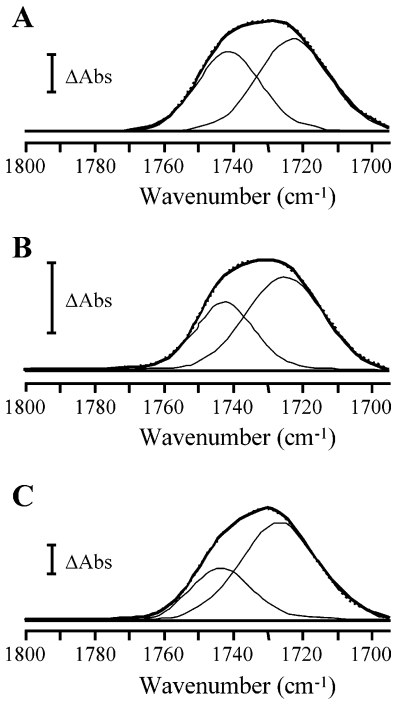

FIGURE 5: Infrared spectra from the C═O carbonyl stretching vibration mode of diester phospholipids: (A) pure POPA in pH 7.4 buffer, (B) POPA in the presence of C2-PKCϵ in pH 7.4 buffer, and (C) pure POPA in pH 10 buffer. The fitted component bands are shown, and the dashed lines correspond to the curve-fitted spectrum; i.e., the dotted lines are the sum of individual components. ΔAbs was 0.01 in panels A and B and 0.02 absorbance unit in panel C.

IR Spectroscopy Study of the Lipid−Water Interface. To better characterize the interaction of the protein with the phospholipids, infrared spectroscopy was used to monitor several important groups in the phospholipid molecule. The C═O carbonyl stretching vibration mode of diester phospholipids appeared in the region of 1700−1760 cm^{-1}. Pure POPA, at 30 °C, exhibited a broad C═O carbonyl band which, after second derivation and band fitting, revealed the presence of two components, one at 1742 cm^{-1} (44%) and another at 1723 cm^{-1} (56%) (Figure 5A). As suggested by Blume et al. (*47*), the component occurring at the higher frequency can be attributed to unhydrated C═O groups, whereas the other component can be assigned to hydrated C═O groups. It has been described that the interaction of other molecules with phospholipids may change the proportion of both types of components and hence the hydration of the carbonyl groups (*37*, *48*). This was also observed to be the case for C2-PKCϵ, and when this protein was added to POPA vesicles, there was a clear change in the profile of the carbonyl band, the component appearing at 1742 cm^{-1} showing a much reduced area (37%) and the component at 1725 cm^{-1} increasing its area quite considerably (63%). This change indicates a substantial change in the conformation of the polar head group of POPA, with an increase in the percentage of hydrated C═O groups as a consequence of the presence of the protein (Figure 5B). Note that the

observed change is exactly the opposite of what was observed for phosphatidic acid when Ca^{2+} ions were added, in which case the higher component increased quite considerably (*49*). However, this change is similar to that previously observed for other proteins interacting with phosphatidic acid, such as bovine myelin basic protein (*50*) and cardiotoxin (*51*). Figure 5C also shows that when POPA became more dissociated, which occurred at pH 10, the components were located at 1742 (31%) and 1725 cm^{-1} (69%).

The other part of the spectrum that was examined was that between 1300 and 1000 cm^{-1}, where the phosphate group vibrations give way to two bands in the infrared spectrum, located at ~1178 cm^{-1}, which can be assigned to the PO_2^- antisymmetric stretching mode, and another at 1077 cm^{-1}, which mainly corresponds to the symmetric stretching vibration, although this last band is rather complex because several other vibrations overlap here (*49*). With respect to the antisymmetric stretching vibration, it is interesting that in phosphatidic acids this band appears at lower wavenumbers than in other phospholipids, such as phosphatidylcholine or phosphatidylserine, where it is found at approximately 1220 cm^{-1}. The hydrogen bonding of the POPA molecules, among themselves, is responsible for this low wavenumber. To observe the effect of the protein on this part of the spectrum, the spectrum of pure POPA and that of POPA with protein were normalized by relation to the CH_2 antisymmetric band appearing at 2854 cm^{-1}, which can be attributed almost exclusively to lipids. We observed that the intensity of this phosphate band decreased as a consequence of the presence of the protein, indicating that the proportion of PO_2^- decreased in favor of PO_2^{2-} (not shown), although the wavenumber at which this band appeared remained unchanged.

With respect to the band at 1077 cm^{-1}, which can be assigned to the symmetric stretching of the PO_2^- group (*49*), this band arises not only from the symmetric stretching vibration of the phosphate group but also from the C−O−(P), P−O−(C), and P−O(H) stretching modes which are quite sensitive to the charge density of the phosphate group (*49*). The addition of the protein clearly changes the shape of the band (not shown); however, the pure protein also absorbs in this part of the spectrum, and given the complexity of the band, additional conclusions should not be drawn.

It should be pointed out that it is not possible to quantify the effect detected here by IR spectroscopy in terms of percentages of lipid molecules affected by the presence of the protein. Only a qualitative view can be obtained, indicating that a number of molecules are affected.

DISCUSSION

Many extrinsic proteins use electrostatic forces to interact with membranes, and they differ from those of intrinsic proteins which interact with membranes mainly through hydrophobic interactions (*52*). Among the extrinsic proteins which establish interactions with membranes and which have been extensively studied, we may mention cytochrome *c* (*29*, *46*, *53*−*55*), myelin basic protein (*46*, *56*, *57*), phospholipases (*58*, *59*), protein kinases C (*60*, *61*), K-Ras (*62*), charybdotoxin (*63*), cardiotoxin (*30*), and Aβ peptides (*31*, *40*, *64*), some of which have been studied by MAS NMR (*29*−*31*, *40*, *54*).

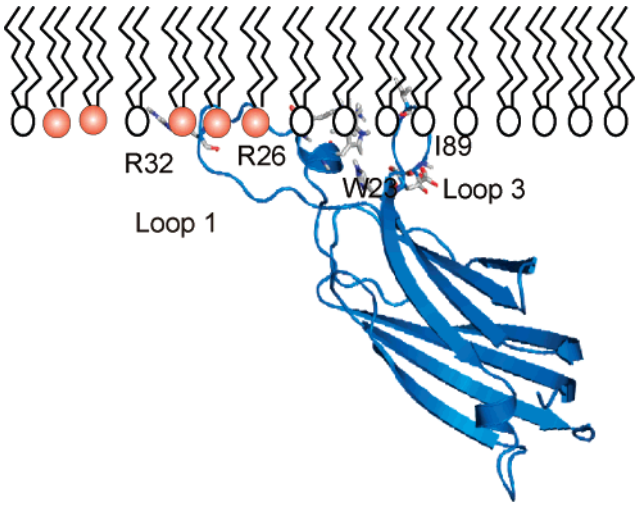

FIGURE 6: Model structure of the lipid binding area of C2-PKCϵ. This model is based on the crystal structure determined by Ochoa et al. (*22*) and is taken from PDB entry 1GMI. Side chains of the residues possibly involved in lipid binding are depicted. According to this model, the docking in the membrane involves electrostatic interaction of R26 and R32 with negatively charged phospholipids (red) which will be reinforced by the insertion of I89 into the hydrophobic palisade and insertion of W23 into the water−lipid interface.

Many proteins involved in signal transduction are activated by their translocation to membranes (*59*, *61*, *62*). Most of these proteins translocate to the plasma membrane, where they bind to negatively charged phospholipids located in the face of the membrane facing the cytoplasm. This is made possible by the asymmetrical disposition of lipids in membranes, which, for example, prevents the binding of blood proteins to blood cells, thus preventing inadequate blood coagulation.

Signal transduction-related proteins which bind electrostatically to membranes include proteins bearing C2 domains, such as PKCs (*60*, *61*), and synaptotagmins (*65*). In the case of Ca^{2+}-dependent C2 domains, Ca^{2+} acts as a bridge between negatively charged phospholipids such as phosphatidylserine and amino acid residues of the protein which is the case with the well-described C2 domain from PKCα (*17*, *18*). Nevertheless, these C2 domains may also establish direct electrostatic interactions with phospholipids like PIP_2 through positively charged residues, such as lysines (*66*).

However, C2 domains from novel PKCs, for example, from PKCϵ, have not been studied so well, although it is known that they do not interact with Ca^{2+} but directly between aminoacyl residues and phospholipids. Previous work using X-ray diffraction and site-directed mutagenesis (*22*, *23*, *25*) showed that interaction may take place through residues W23, R26, and R32 located in loop 1 and I89 located in loop 3, the interaction being predominantly electrostatic (*23*). Figure 6 depicts a docking of the protein in a membrane, which reflects the observations made in this paper, with W23 localized in the water−lipid interface and R26 and R32 interacting with negatively charged phospholipids (depicted with a red head). Note that I89 penetrates through its lateral chain in the hydrophobic palisade, accounting for the fact that its mutation seriously disrupts the interaction of C2-PKCϵ with the membrane (*22*).

Our study confirms that the main way in which C2-PKCϵ interacts with membranes is electrostatic in nature, with a very small contribution on the part of hydrophobic interactions, as indicated by DSC. The MAS NMR experiments described in this paper clearly demonstrate that C2-PKCϵ electrostatically interacts with POPA much more than with POPC. This is indicated by the downfield shift in the isotropic resonance of POPA and the widening of the resonance peak, so the fwhh clearly increased. This reflected a decrease in the mobility of the phospholipids, as confirmed by the decrease in T_2 and by the decrease observed in T_1 at all temperatures. All these effects were much more pronounced than the very small effect observed for POPC, indicating the specificity of the interaction.

The mutant PKCϵ-C2W23A/R26A/R32A was a good control which demonstrated that, following the elimination of positively charged residues, the effect on the phosphate group of POPA is reduced.

It is interesting that the addition of POPC to POPA led to an increase in T_1, which may have been the result of interactions between the negatively charged head groups, the intercalation of POPC molecules breaking these interactions. The reduction in T_1 induced by the presence of the protein at all temperatures (Figure 4) reflects a more efficient relaxation mechanism. These results confirm the specificity of the protein in its effect on POPA, while the decrease in T_1 indicates restrictions in headgroup motion that lower the spectral density of fast motions of the phosphorus atoms.

If we compare the effect of C2-PKCϵ with that produced by Ca^{2+} ions, it can be seen that the latter dramatically increase the value of T_1 (*67*). Like other proteins such as cytochrome *c*, C2-PKCϵ behaves more like monovalent cations and some divalent cations that act as counterions within the electrical double layer (*68*, *70*). This type of effect is quite compatible with the lack of phase separation observed by DSC following the addition of protein to POPC/POPA mixtures.

The binding of C2-PKCϵ induces an increase in the level of ionization of the PO_2^- group of POPA, as seen by IR spectroscopy, this changing the conformation of at least some phospholipid head groups, as shown through the increase in the percentage of hydration of the carbonyl group of POPA. Notice also that the increase in the chemical shifts of the isotropic ^{31}P NMR resonances confirms the strengthened dissociation of the phosphoryl group of POPA and hence a decrease in the apparent pK_a of this chemical group (*38*, *39*). Phosphatidic acid is a very special phospholipid since it is the only one which possesses a pK_a in the physiological range, and its protonated state may change as a function of its interaction with other lipids or proteins (*38*, *39*). These interactions usually involve hydrogen bonding, and this may be important in determining its various cellular functions.

To interpret the results we obtained, we should take into account the fact that no phase separation between POPC and POPA was observed in DSC and that all of the POPA lipid molecules exhibited homogeneous downfield chemical shifts and altered T_1 values for their ^{31}P NMR resonances after protein binding, although a 40:1 lipid:protein molar ratio was used. Two populations of POPA molecules are not observed, but instead, a small number of protein molecules alter the environment of a much larger number of lipid molecules. If these observed bulk perturbations were due to the binding of protein to the lipid headgroup, then the system must be at the rapid exchange limit, wherein each lipid is visited by one or more proteins on a NMR time scale. Since this time scale can be assumed to be around $10^{-4}-10^{-5}$ s, this technique cannot separate two states exchanging at a rate faster than $\sim 10^4-10^5$ s^{-1}. Since the lateral diffusion of lipids in a fluid membrane tells us that the time needed for a phospholipid to exchange its position with an adjacent one is $\sim 10^{-7}$ s (*71*), it is feasible that 40 phospholipid molecules could visit a protein, and still only one single type of lipid would be detected. Note that the T_1 values (Figure 4) would be averages, and the T_1 values of POPA molecules actually bound to proteins would be smaller than the observed values. This situation is similar to that found for the interaction of phospholipids with intrinsic membrane proteins (*52*).

The other possibility is that a low density of protein molecules bound to the membrane surface could alter the environments of all the headgroups simultaneously by driving a conformational rearrangement of these headgroups. Such a global conformational rearrangement could alter the headgroup pK_a value, which would, in turn, alter the chemical shift and relaxation values. The IR data may be taken to support the second interpretation. It is clear that the binding of the protein generates an overall change in the conformation of the lipid headgroups, which could account for the bulk effects on the NMR parameters observed for the POPA population. However, when the IR data are being considered, it is not possible to quantify the effect in terms of the percentage of lipid molecules affected, and therefore, we cannot exclude the rapid dissociation model to explain our results.

Our data could support a model in which some positively charged residues of the protein will alter the diffuse double layer of the membrane, inducing an alteration of the apparent pK_a of POPA, which can be deduced from the downfield movement of the ^{31}P NMR isotropic chemical shift and from the infrared data. However, we cannot exclude the possibility that some lipids could be bound to the protein at a given moment, rapidly moving (with respect to the time scale of the experiment) in and out.

Therefore, it could be that both interpretations are partially true and that not all the lipid molecules are affected by the protein at the same time; on the other hand, not only those directly contacting the protein would be affected at a given moment.

It should also be mentioned that the T_2 spin−spin relaxation times corroborate the observed widening of the isotropic ^{31}P NMR resonances (Table 2). The most likely explanation seems to be a reduced lipid mobility with respect to the bilayer, affecting especially POPA due to its sensitivity to the presence of the protein. We have no experimental evidence due to the existence of microenvironments, derived, for example, from different local densities of bound protein.

In summary, C2-PKCϵ shows a preference for POPA over POPC, while electrostatic interaction which is established changes the conformation of the polar headgroup of POPA. These observations confirm the role of phosphatidic acid in activating PKCϵ as suggested by recent in vivo studies (*25*) so that this enzyme may be also regulated through phospholipase D activity.

REFERENCES

1. Brodie, C., Bogi, K., Acs, P., Lazarovici, P., Petrovics, G., Anderson, W. B., and Blumberg, P. M. (1999) Protein kinase C-ϵ plays a role in neurite outgrowth in response to EGF and NGF in PC12 cells, *Cell Growth Differ. 10*, 183−191.
2. Zeidman, R., Lofgren, B., Pahlman, S., and Larsson, C. (1999) PKCϵ, via its regulatory domain and independently of its catalytic domain, induces neurite like processes in neuroblastoma cells, *J. Cell Biol. 145*, 713−726.
3. Pfeffer, L. M., Eisenkraft, B. L., Reich, N. C., Improta, T., Baxter, G., Daniel, S., Issakani, S., and Strulovici, B. (1991) Transmembrane signaling by interferon α involves diacylglycerol production and activation of the ϵ isoform of protein kinase C in Daudi cells, *Proc. Natl. Acad. Sci. U.S.A. 88*, 7988−7992.
4. Akita, Y., Ohno, S., Yajima, Y., Konno, Y., Saido, T. C., Mizuno, K., Chida, K., Osada, S., Kuroki, T., and Kawashima, S. (1994) Overproduction of a Ca^{2+}-independent protein kinase C isozyme, nPKC ϵ, increases the secretion of prolactin from thyrotropin-releasing hormone-stimulated rat pituitary GH4C1 cells, *J. Biol. Chem. 269*, 4653−4660.
5. Lehel, C., Olah, Z., Mischack, H., Mushinski, J. F., and Anderson, W. B. (1994) Overexpressed protein kinase C-δ and -ϵ subtypes in NIH 3T3 cells exhibit differential subcellular localization and differential regulation of sodium-dependent phosphate uptake, *J. Biol. Chem. 269*, 4761−4766.
6. Liedtke, C. M., Yun, C. H. C., Kyle, N., and Wang, D. (2002) PKC ϵ-dependent regulation of cystic fibrosis transmembrane regulator involves binding to a receptor for RACK1 and RACK1 binding to Na^+/H^+ exchange regulatory factor, *J. Biol. Chem. 277*, 22925−22933.
7. Ivaska, J., Whelan, R. D. H., Watson, R., and Parker, P. J. (2002) PKCϵ controls the traffic of β1-integrins in motile cells, *EMBO J. 21*, 3608−3619.
8. Ivaska, J., Bosca, L., and Parker, P. J. (2003) PKCϵ is a permissive link in integrin-dependent IFN-γ signalling that facilitates JAK phosphorylation of STAT1, *Nat. Cell Biol. 5*, 363−369.
9. Basu, A., Lu, D., Sun, B., Moor, A. N., Akkaraju, G. R., and Huang, J. (2002) Proteolytic activation of protein kinase C-ϵ by caspase-mediated processing and transduction of antiapoptotic signals, *J. Biol. Chem. 277*, 41850−41856.
10. Comalada, M., Xaus, J., Valledor, A. F., Lopez-Lopez, C., Pennington, D. J., and Celada, A. (2003) PKC ϵ is involved in JNK activation that mediates LPS-induced TNF-α, which induces apoptosis in macrophages, *Am. J. Physiol. 285*, C1235−C1245.
11. Jung, Y. S., Ryu, B. R., Lee, B. K., et al. (2004) Role for PKC-ϵ in neuronal death induced by oxidative stress, *Biochem. Biophys. Res. Commun. 320*, 789−794.
12. Liu, G., Cohen, M., Mochly-Rosen, D., and Downey, J. (1999) Protein kinase Cϵ is responsible for the protection of preconditioning in rabbit cardiomyocytes, *J. Mol. Cell. Cardiol. 31*, 1937−1948.
13. Cross, H. R., Murphy, E., Bolli, R., Ping, P., and Steenbergen, C. (2002) Expression of activated PKC ϵ (PKCϵ) protects the ischaemic heart, without attenuating ischaemic H^+ production, *J. Mol. Cell. Cardiol. 34*, 361−367.
14. Malhotra, A., Begley, R., Kang, B. P., Rana, I., Liu, J., Yang, G., Mochly-Rosen, D., and Meggs, L. G. (2005) PKC-ϵ-dependent survival signals in diabetic hearts, *Am. J. Physiol. 289*, 1343−1350.
15. Inagaki, K., Begley, R., Ikeno, F., and Mochly-Rosen, D. (2005) Cardioprotection by ϵ-protein kinase C activation from ischemia: Continuous delivery and antiarrhythmic effect of an ϵ-protein kinase C-activating peptide, *Circulation 111*, 44−50.
16. Corbalán-García, S., Rodríguez-Alfaro, J. A., and Gómez-Fernández, J. C. (1999) Determination of the calcium-binding sites of the C2 domain of protein kinase Cα that are critical for its translocation to the plasma membrane, *Biochem. J. 337*, 513−521.
17. Ochoa, W. F., Corbalán-García, S., Eritja, R., Rodriguez-Alfaro, J. A., Gómez-Fernández, J. C., Fita, I., and Verdaguer, N. (2002) Additional binding sites for anionic phospholipids and calcium ions in the crystal structures of complexes of the C2 domain of protein kinase Cα, *J. Mol. Biol. 320*, 277−291.
18. Verdaguer, N., Corbalán-García, S., Ochoa, W. F., Fita, I., and Gómez-Fernández, J. C. (1999) Ca^{2+} bridges the C2 membrane-binding domain of protein kinase Cα directly to phosphatidylserine, *EMBO J. 18*, 6329−6338.
19. Hernandez-Caselles, T., Villalain, J., and Gomez-Fernandez, J. C. (1993) Influence of liposome charge and composition on their interaction with human blood serum proteins, *Mol. Cell. Biochem. 120*, 119−126.
20. Medkova, M., and Cho, W. (1998) Mutagenesis of the C2 domain of protein kinase Cϵ, *J. Biol. Chem. 273*, 17544−17552.
21. García-García, J., Gómez-Fernández, J. C., and Corbalán-García, S. (2001) Structural characterization of the C2 domain of novel protein kinase Cϵ, *Eur. J. Biochem. 268*, 1107−1117.
22. Ochoa, W. F., García-García, J., Fita, I., Corbalán-García, S., Verdaguer, N., and Gómez-Fernández, J. C. (2001) Structure of the C2 domain from novel protein kinase Cϵ. A membrane binding model for Ca^{2+}-independent C2 domains, *J. Mol. Biol. 311*, 837−849.
23. Corbalán-García, S., Sánchez-Carrillo, S., García-García, J., and Gómez-Fernández, J. C. (2003) Characterization of the membrane binding mode of the C2 domain of PKCϵ, *Biochemistry 42*, 11661−11668.
24. Stahelin, R. V., Digman, M. A., Medkova, M., Ananthanarayanan, B., Melowic, H. R., Rafter, J. D., and Cho, W. (2005) Diacylglycerol-induced membrane targeting and activation of protein kinase Cϵ: Mechanistic differences between protein kinases Cα and Cα, *J. Biol. Chem. 280*, 19784−19793.
25. López-Andreo, M. J., Gómez-Fernández, J. C., and Corbalán-García, S. (2003) The simultaneous production of phosphatidic acid and diacylglycerol is essential for the translocation of protein kinase Cϵ to the plasma membrane in RBL-2H3 cells, *Mol. Biol. Cell 14*, 4885−4895.
26. Testerink, C., and Munnik, T. (2005) Phosphatidic acid: A multifunctional stress signalling lipid in plants, *Trends Plant Sci. 10*, 368−375.
27. Oldfield, E., Bowers, J. L., and Forbes, J. (1987) High resolution proton and carbon-13 NMR of membranes: Why sonicate? *Biochemistry 26*, 6919−6923.
28. Hamilton, J. A., Fujito, D. T., and Hammer, C. F. (1991) Solubilization and localization of weakly polar lipids in unsonicated egg phosphatidylcholine: A ^{13}C MAS NMR study, *Biochemistry 30*, 2894−2902.
29. Pinheiro, T. J., and Watts, A. (1994) Resolution of individual lipids in mixed phospholipid membranes and specific lipid-cytochrome c interactions by magic-angle solid-state phosphorus-31 NMR, *Biochemistry 33*, 2459−2467.
30. Carbone, M. A., and Macdonald, P. M. (1996) Cardiotoxin II segregates phosphatidylglycerol from mixtures with phosphatidylcholine: ^{31}P and ^{2}H NMR spectroscopic evidence, *Biochemistry 35*, 3368−3378.
31. Bonev, B., Watts, A., Bokvist, M., and Gröbner, G. (2001) Electrostatic peptide−lipid interactions of amyloid-β peptide and pentalysine with membrane surfaces monitored by P-31 MAS NMR, *Phys. Chem. Chem. Phys. 3*, 2904−2910.
32. Bonev, B. B., Lam, Y.-H., Anderluh, G., Watts, A., Norton, R. S., and Separovic, F. (2003) Effects of the eukaryotic pore-forming cytolysin equinatoxin II on lipid membranes and the role of sphyngomyelin, *Biophys. J. 84*, 2382−2392.
33. Lindström, F., Williamson, P. T. F., and Gröbner, G. (2005) Molecular insight into the electrostatic membrane surface potential by $^{14}N/^{31}P$ MAS NMR spectroscopy: Nociceptin-lipid association, *J. Am. Chem. Soc. 127*, 6610−6616.
34. Saiki, R. K., Gelfan, D. H., Stoftel, S., Scharf, S. J., Higuchi, R., Horn, G. T., Mullis, K. B., and Erlich, H. A. (1988) Primer-directed enzymatic amplification of DNA with a thermostable DNA polymerase, *Science 235*, 487−491.
35. Smith, P. K., Krohn, R. I., Hermanson, G. T., Mallia, A. K., Gartner, F. H., Provenzano, M. D., Fujimoto, E. K., Goeke, N. M., Olson, B. J., and Klenk, D. C. (1985) Measurement of protein using bicinchoninic acid, *Anal. Biochem. 150*, 76−85.
36. Chapman, D., Gómez-Fernández, J. C., Goñi, F. M., and Barnard, M. (1980) Difference infrared spectroscopy of aqueous model and biological membranes using an infrared data station, *J. Biochem. Biophys. Methods 2*, 315−323.
37. López-García, F., Micol, V., Villalaín, J., and Gómez-Fernández, J. C. (1993) Infrared spectroscopic study of the interaction of diacylglycerol with phosphatidylserine in the presence of calcium, *Biochim. Biophys. Acta 1169*, 264−272.
38. Swairjo, M. A., Seaton, B. A., and Roberts, M. F. (1994) Effect of vesicle composition and curvature on the dissociation of phosphatidic acid in small unilamellar vesicles: A ^{31}P-NMR study, *Biochim. Biophys. Acta 1191*, 354−361.

39. Kooijman, E. E., Carter, K. M., van Laar, E. G., Chupin, V., Burger, K. N., and de Kruijff, B. (2005) What makes the bioactive lipids phosphatidic acid and lysophosphatidic acid so special? *Biochemistry 44*, 17007−17015.
40. Bokvist, M., Lindstrom, F., Watts, A., and Grobner, G. (2004) Two types of Alzheimer's β-amyloid(1−40) peptide membrane interactions: Aggregation preventing transmembrane anchoring versus accelerated surface fibril formation, *J. Mol. Biol. 335*, 1039−1049.
41. Tamm, L. K., and Seelig, J. (1983) Lipid salvation of cytochrome c oxidase. Deuterium, nitrogen-14, and phosphorus-31 nuclear magnetic resonance studies on the phosphocholine head group and on cis-unsaturated fatty acyl chains, *Biophys. J. 22*, 1474−1483.
42. Seelig, J., Tamm, L., Hymel, L., and Fleischer, S. (1981) Deuterium and phosphorus nuclear magnetic resonance and fluorescence depolarization studies of functional reconstituted sarcoplasmic reticulum membrane vesicles, *Biochemistry 20*, 3922−3932.
43. Spooner, P. J., and Watts, A. (1991) Reversible unfolding of cytochrome c upon interaction with cardiolipin bilayers. 2. Evidence from phosphorus-31 NMR measurements, *Biochemistry 30*, 3880−3885.
44. Harlos, K., Eibl, H., Pascher, I., and Sundell, S. (1984) Conformation and packing properties of phosphatidic acid: The crystal structure of monosodium dimyristoylhosphatidate, *Chem. Phys. Lipids 34*, 115−126.
45. Waltham, M. C., Cornell, B. A., and Smith, R. (1986) Association of ferri- and ferro-cytochrome c with lipid multibilayers: A ^{31}P solid-state NMR study, *Biochim. Biophys. Acta 862*, 451−456.
46. Smith, R., Cornell, B. A., Keniry, M. A., and Separovic, F. (1983) ^{31}P nuclear magnetic resonance studies of the association of basic proteins with multilayers of diacyl phosphatidylserine, *Biochim. Biophys. Acta 732*, 492−498.
47. Blume, A., Hubner, W., and Messner, G. (1988) Fourier transform infrared spectroscopy of ^{13}C═O labelled phospholipids. Hydrogen bonding to carbonyl groups, *Biochemistry 27*, 8299−8249.
48. López-García, F. J., Villalaín, J., Gómez-Fernández, J. C., and Quinn, P. J. (1994) The phase behaviour of mixed aqueous dispersions of dipalmitoyl derivatives of phosphatidylcholine and diacylglycerol, *Biophys. J. 66*, 1991−2004.
49. Laroche, G., Dufourc, E. J., Dufourcq, J., and Pezolet, M. (1991) Structure and dynamics of dimyristoylphosphatidic acid/calcium complexes by ^{2}H NMR, infrared, spectroscopies and small-angle x-ray diffraction, *Biochemistry 30*, 3105−3114.
50. Nabet, A., Boggs, J. M., and Pezolet, M. (1994) Study by infrared spectroscopy of the interaction of bovine myelin basic protein with phosphatidic acid, *Biochemistry 33*, 14792−14799.
51. Desormeaux, A., Laroche, G., Bougis, P. E., and Pezolet, M. (1992) Characterization by infrared spectroscopy of the interaction of a cardiotoxin with phosphatidic acid and with binary mixtures of phosphatidic acid and phosphatidylcholine, *Biochemistry 31*, 12173−12182.
52. Chapman, D., Gómez-Fernández, J. C., and Goñi, F. M. (1982) The interaction of intrinsic proteins and lipids in biomembranes, *Trends Biochem. Sci. 7*, 67−70.
53. Rietveld, A., Berkhout, T. A., Roenhorst, A., Marsh, D., and de Kruijff, B. (1986) Preferential association of apocytochrome c with negatively charged phospholipids in mixed model membranes, *Biochim. Biophys. Acta 858*, 38−46.
54. Pinheiro, T. J., and Watts, A. (1994) Lipid specificity in the interaction of cytochrome c with anionic phospholipid bilayers revealed by solid state ^{31}P-NMR, *Biochemistry 33*, 2451−2458.
55. Rytomaa, M., and Kinnunen, P. K. J. (1995) Reversibility of the binding of cytochrome to liposomes. Implications for lipid-protein interactions, *J. Biol. Chem. 270*, 3197−3202.
56. MacNaughtan, W., Snook, K. A., Caspi, E., and Franks, N. P. (1985) An X-ray diffraction analysis of oriented lipid multilayers containing basic proteins, *Biochim. Biophys. Acta 818*, 132−148.
57. Jo, E., and Boggs, J. M. (1995) Aggregation of acidic lipid vesicles by myelin basic protein: Dependence on potassium concentration, *Biochemistry 34*, 13705−13716.
58. Rebecchi, M., Peterson, A., and McLaughlin, S. (1992) Phosphoinositide-specific phospholipase C-δ 1 binds with high affinity to phospholipid vesicles containing phosphatidylinositol 4,5-bisphosphate, *Biochemistry 31*, 12742−12747.
59. Roberts, M. F. (1996) Phospholipases: Structural and functional motifs for working at an interface, *FASEB J. 10*, 1159−1172.
60. Newton, A. C., and Johnson, J. E. (1998) Protein kinase C: A paradigm for regulation of protein function by two membrane-targeting modules, *Biochim. Biophys. Acta 1376*, 155−172.
61. Corbalán-García, S., and Gómez-Fernández, J. C. (2006) Protein kinase C regulatory domains: The art of decoding many different signals in membranes, *Biochim. Biophys. Acta 1761*, 633−654.
62. Hancock, J. F., Paterson, H., and Marshall, C. J. (1990) A polybasic domain or palmitoylation is required in addition to the CAAX motif to localize p21ras to the plasma membrane, *Cell 6*, 133−139.
63. Ben-Tal, N., Honig, B., Miller, C., and McLaughlin, S. (1997) Electrostatic binding of proteins to membranes. Theoretical predictions and experimental results with charybdotoxin and phospholipid vesicles, *Biophys. J. 73*, 1717−1727.
64. Martinez-Senac, M. d. M., Villalaín, J., and Gómez-Fernández, J. C. (1999) Structure of the Alzheimer β-amyloid peptide(25−35) and its interaction with negatively charged phospholipid vesicles, *Eur. J. Biochem. 265*, 744−753.
65. Bai, J., and Chapman, E. R. (2004) The C2 domains of synaptotagmin: Partners in exocytosis, *Trends Biochem. Sci. 29*, 143−145.
66. Corbalán-García, S., García-García, J., Rodríguez-Alfaro, J. A., and Gómez-Fernández, J. C. (2003) A new phosphatidylinositol 4,5-bisphosphate-binding site located in the C2 domain of protein kinase Cα, *J. Biol. Chem. 278*, 4972−4980.
67. Hope, M. J., and Cullis, P. R. (1980) Effects of divalent cations and pH on phosphatidylserine model membranes: A ^{31}P NMR study, *Biochem. Biophys. Res. Commun. 92*, 846−852.
68. Portis, A., Newton, C., Pangborn, W., and Papahadjopoulos, D. (1979) Studies on the mechanism of membrane fusion: Evidence for an intermembrane Ca^{2+}-phospholipid complex, synergism with Mg^{2+}, and inhibition by spectrin, *Biochemistry 18*, 780−790.
69. Puskin, J. S., and Coene, M. T. (1980) Na^{+} and H^{+} dependent Mn^{2+} binding to phosphatidylserine vesicles as a test of the Gouy-Chapman-Stern theory, *J. Membr. Biol. 52*, 69−74.
70. McLaughlin, S. (1989) The electrostatic properties of membranes, *Annu. Rev. Biophys. Biophys. Chem. 18*, 113−136.
71. Träuble, H., and Sackmann, E. (1972) Studies of the crystalline-liquid crystalline phase transition of lipid model membranes. 3. Structure of a steroid-lecithin system below and above the lipid-phase transition, *J. Am. Chem. Soc. 94*, 4499−4510.

BI0621720